# Solvent-Responsive Behavior of Inclusion Complexes Between Amylose and Polytetrahydrofuran

Rachmawati, R; Woortman, Albert; Loos, Katja

*Published in:*
Macromolecular Bioscience

*DOI:*
10.1002/mabi.201300174



*Publication date:*
2014

# Solvent-Responsive Behavior of Inclusion Complexes Between Amylose and Polytetrahydrofuran[a]

Rachmawati Rachmawati, Albert J. J. Woortman, Katja Loos*

Highly crystalline amylose–polytetrahydrofuran (PTHF) complexes can be obtained by employing organic solvents as washing agents after complex formation. The X-ray diffraction (XRD) of the washed complexes appear sharp at 12.9°–13.2° and 19.6°–20.1°, clear signs of the presence of $V_{6I}$-amylose. Other diffraction peaks correlate with $V_{6II}$-amylose, which indicates that the complexed amylose helices are in the form of an intermediate or a mixture of $V_{6I}$- and $V_{6II}$-amylose. SEM imaging reveals that the amylose–PTHF complexes crystallize in the form of lamellae, which aggregate in a round shape on top of one another with a diameter around 4–8 μm. Some lamellas aggregate as flower-like or flat-surface spherulitic crystals. There is a visible matrix in between the aggregated lamellas which shows that a part of the amylose–PTHF complexes is amorphous.

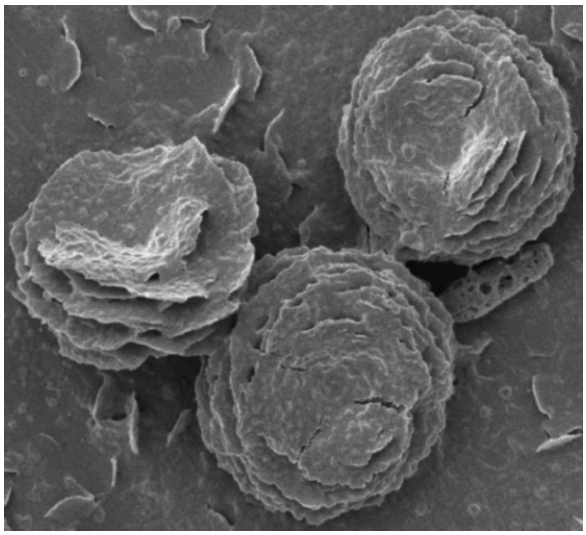

## 1. Introduction

Amylose is a linear polysaccharide, which is able to include suitable guest molecules into its helix chains to form complexes. The guest molecules range from small molecules such as iodine,[1,2] alcohols,[3,4] lipids,[5–7] and fatty acids,[8,9] to big molecules such as polymers.[10–23] As polymers are lengthy molecules, certain aspects have to be considered to compensate the fact that the formation of the complexes is mainly based on hydrophobic interactions. This includes the hydrophobicity of the polymer backbone, the functional groups of the head–tail or the side chain of the polymer.[10–25]

The non-covalent interactions between amylose and guest molecules offer interesting properties, which can lead to solvent- and temperature-responsive materials. In this case, the type and the location of the guest molecules (inside and/or in between the amylose helices) play important roles. In combination with the nature of amylose, such as its biodegradability and its facile synthesis via enzymatic polymerization,[26–30] amylose inclusion complexes open a facile route to supramolecular chemistry.

Dr. R. Rachmawati, A. J. J. Woortman, Prof. K. Loos
Department of Polymer Chemistry, Zernike Institute for Advanced Materials, University of Groningen, Nijenborgh 4, 9747AG Groningen, The Netherlands
E-mail: k.u.loos@rug.nl

[a]**Supporting Information** is available at Wiley Online Library or from the author.




DOI: 10.1002/mabi.201300174

As crystalline materials, the amylose inclusion complexes mostly crystallize in the form of lamellae, which is caused by the folding of amylose chains.[31,32] Some guest molecules such as butanol[33] and lactone[34] can form inclusion complexes with amylose in starch and crystallize in the form of a distinctive spherulite. In the case of amylose–lipid complexes, the complexes can be arranged in a fringed micellar organization or by folding into U-shapes.[6] As more interactions are possible in the fringed micellar organization especially for long amylose chains, the resulting complex can crystallize as a network of lamellae interconnected by amorphous amylose.[6] The amorphous part is mostly correlated to the unwinded amylose helix, which can be caused by the rupture of the hydrogen bonds or by the guest-free void within the amylose helix.[6,35] Another example is the complex between amylose and α-naphthol which crystallizes in the form of a cushion-shaped single crystal, or in the form of pseudo-spherocrystals.[36] The resulted morphologies depend greatly on the concentration, heating and recrystallization temperature of the complexes.[36]

Guest molecules which reside in between the amylose helices, such as isopropanol/acetone[32] or *n*-butanol/*n*-pentanol,[4] undergo dissolution in ethanol. Upon dissolution, the resulted crystals of the complexes were reported to change, namely from a $V_7$- to $V_h$-amylose (or $V_7$- to $V_{6I}$-amylose) in the case of amylose–isopropanol/acetone complexes[32] and from $V_{6II}$- to $V_{6I}$-amylose in the case of amylose–*n*-butanol/*n*-pentanol complexes.[4]

Amylose–polytetrahydrofuran (PTHF) complexes have been previously reported to being arranged as a mixture or an intermediate between $V_{6I}$- and $V_{6II}$-amylose.[24,25] In this case, there is a possibility that the included PTHF can undergo dissolution in suitable solvents which can lead to the change on the corresponding structure of the amylose–PTHF complexes. To study the effects of the dissolution, some solvents such as ethanol, THF, chloroform, and dichloromethane were used as washing agents for amylose–PTHF complexes. The solvents were expected to remove the PTHF chains located in between the amylose helices and some other loosely bound PTHFs. PTHFs with a molecular weight of 650 and 1000 g mol$^{-1}$ were used as guest polymers as they have a high complexing ability with amylose.[24,25]

The exact crystal structure of the amylose–polymer complexes has not been reported. As a crystal structure determination usually requires a single crystal of the complex, one of the aims of this study is to firstly investigate the morphology of the resulting amylose–PTHF complexes. In addition, to investigating the morphology of amylose–PTHF complexes, scanning electron microscopy (SEM) was used to image the structures of the washed complexes. Because amylose with high molecular weight was used ($M_v$ ≈ 200 kg mol$^{-1}$) for the complexation, it is expected that the resulting complexes will not crystallize as a single crystal.

## 2. Experimental Section

### 2.1. Materials

Amylose with a molecular weight ($M_v$) of ≈200 kg mol$^{-1}$ (amylose, from Avebe), hydroxyl terminated PTHF with molecular weights of 650 and 1000 g mol$^{-1}$ (PTHF650 and PTHF1000, from Aldrich), ethanol (EtOH, >99.9%, from Emsure), tetrahydrofuran (THF, >99.5%, from Acros), chloroform ($CHCl_3$, 99.5%, from LAB-SCAN), dichloromethane ($CH_2Cl_2$, 99.8%, from LAB-SCAN), and potassium carbonate ($K_2CO_3$, >99%, from Merck) were used as received.

### 2.2. Preparation of Amylose–PTHF Complexes

Amylose–PTHF650 complexes were prepared by the method one-pot (OP) for 16 h complexation time, while amylose–PTHF1000 complexes were prepared according to the method OP and the method individual solubilization (IS) for 0, 1, and 16 h complexation time as previously reported.[25] The resulting complexes were diluted at 85 °C to 1% w/v (based on amylose concentration in water). The diluted complexes were centrifuged for 5 min at 2000 rpm at room temperature. The supernatants were thrown away, and the precipitates were washed with hot water and centrifuged for 5 min at 2000 rpm. The precipitates were collected and washed with ethanol. The resulting products were air-dried overnight (ethanol-washed products, herein stated as the E-washed products). The recovery of the E-washed products was around 30–40%, which was calculated gravimetrically based on the total weight of amylose and PTHF. Other concentrations of water/EtOH in combination with different drying methods were also used to wash amylose–PTHF650 complexes as shown in Scheme 1.

### 2.3. Stability Test Toward Solvents

20 mg of 1 h-E-washed amylose–PTHF1000 complexes (prepared by method OP) was suspended in 10 mL THF and shaken for 1 h. The suspension was filtered and washed with THF and air-dried. The same procedure was performed using $CHCl_3$, $CH_2Cl_2$, and THF/EtOH as the solvents and washing agents.

### 2.4. Differential Scanning Calorimetry (DSC)

The measurements were performed on a Perkin Elmer Pyris 1 DSC that had been calibrated with indium. An empty pan was taken as a reference. The samples were weighed into DSC large volume cups (LVCs) as a suspension in water at a concentration of 10% w/w. The samples were equilibrated overnight before the measurement. The samples were heated and cooled under nitrogen in the range of 1–160 °C with a rate of 10 °C min$^{-1}$. The products were calculated as 97% dry matter for freeze-dried samples and 90% for air-dried samples.

### 2.5. X-ray Diffraction (XRD)

The samples were put over saturated $K_2CO_3$ solution for 7 d unless stated otherwise. The measurement was performed on a powder diffractometer (Bruker D8) using $CuK_\alpha$ with a wavelength of 1.54 Å

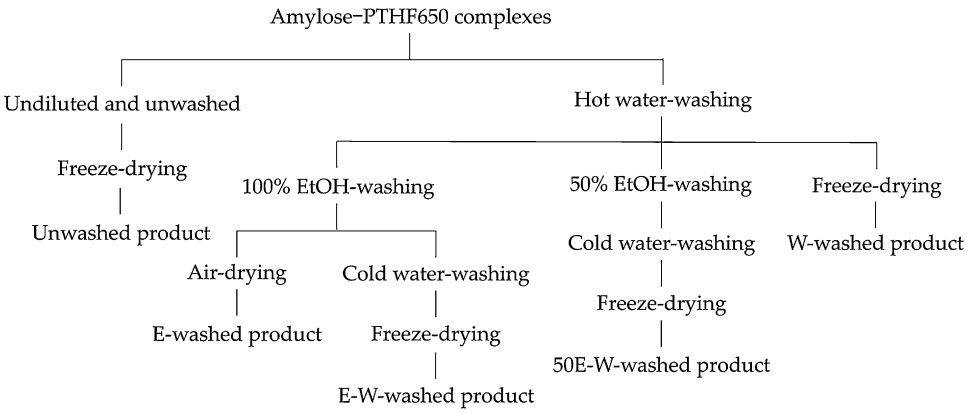


*Scheme 1.* Scheme of purification design of the amylose–PTHF650 complexes. W and E denote water and EtOH, respectively.

as the radiation source. The ranges of $2\theta$ between 5° and 35° were obtained by scanning the samples with interval 0.05° at 8 s per step. The resulting data were smoothed using fast Fourier transform (FFT) filter.

### 2.6. Scanning Electron Microscopy (SEM)

The samples (0.5–1 g $L^{-1}$) were heated to 160 °C and allowed to recrystallize at room temperature, 60 or 85 °C for 1–3 d. The dilute suspensions were then allowed to dry at 40–50 °C (for 30–120 min) or at room temperature overnight. Prior to imaging, the samples were coated with 3 nm platinum/palladium (80:20) alloy. The measurements were performed on a JEOL 6320F Field Emission Microscope operating at 3 kV with a beam current of $1 \times 10^{-10}$ A.

## 3. Results and Discussion

Water is a good washing agent for the purification of amylose–PTHF complexes as it can wash away uncomplexed amylose without washing out included PTHF.[25] However, as there is the possibility that some free PTHF remains, the use of organic solvents such as ethanol is commonly used to purify amylose inclusion complexes.[37–39]

As shown in Figure 1, the unwashed amylose–PTHF650 complex showed the endothermic peaks of the PTHF (between 20 and 40 °C) and the complex (between 110 and 160 °C). The PTHF peak is still visible after water-washing but disappears after ethanol washing. The PTHF peak of the unwashed complex can be a mixture of included and unincluded (free) PTHFs, while the PTHF peak of the water-washed complex (W-washed) relates to the PTHF chains which are located in between the amylose helices.[25] In this case, when ethanol is used as a washing agent, there is the possibility that ethanol washes away both free and some of the included PTHF, which will decrease the amount of the resulting amylose–PTHF complexes. To study the solvent behavior of amylose–PTHF complexes, ethanol with different concentrations and sequences in combination with water and drying methods were used to purify the amylose–PTHF complexes. In addition, other solvents such as THF, chloroform, and dichloromethane were used to rewash the ethanol-washed complexes to investigate the stability of the complexes towards solvents.

Variation on the use of water and ethanol as washing solvents for amylose–PTHF650 complexes.

The DSC data of the resulted amylose–PTHF650 complexes are shown in Table 1. The unwashed and W-washed amylose–PTHF650 complexes show a small melting endotherm of PTHF. The $t_m$'s of the unwashed and W-washed complexes in the first heating scan are comparable (≈134 °C). However, the $\Delta H_m$ of the W-washed complex (≈26 J $g^{-1}$) is slightly higher compared to the unwashed products (≈23 J $g^{-1}$). The small difference in the $\Delta H_m$ is expected as 20% PTHF650 (w/w based on amylose) is almost fully included by the amylose. The difference of the $\Delta H$ is clearer during the first cooling and the second heating, in which the $\Delta H$ of the unwashed/W-washed complex is 19/23 J $g^{-1}$ (first cooling) and 21/24 J $g^{-1}$ (second heating). The

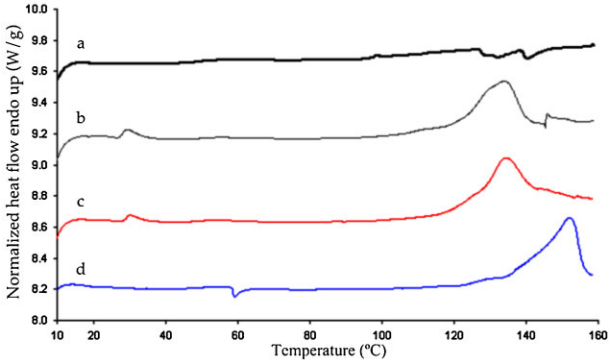


*Figure 1.* DSC thermograms of the first heating scans of a) amylose and b) 16 h-amylose–PTHF650 complexes that were unwashed, c) water-washed, and d) ethanol-washed.

*Table 1.* DSC data of inclusion complexes between amylose and PTHF650.

| | First heating scan | | | | First cooling scan | | | Second heating scan | | |
|---|---|---|---|---|---|---|---|---|---|---|
| | PTHF | Inclusion complexes | | | | | | | | |
| Sample | $\Delta H$ [J g$^{-1}$] | Onset [°C] | Peak [°C] | $\Delta H$ [J g$^{-1}$] | Onset [°C] | Peak [°C] | $\Delta H$ [J g$^{-1}$] | Onset [°C] | Peak [°C] | $\Delta H$ [J g$^{-1}$] |
| Unwashed | 1.5 | 121.8 | 134.0 | 22.5 | 105.8 | 99.6 | −18.6 | 124.7 | 132.5 | 21.4 |
| W-washed | 0.7 | 125.7 | 134.4 | 25.9 | 110.3 | 103.4 | −22.5 | 125.4 | 133.8 | 24.2 |
| E-washed | | 141.9 | 152.3 | 27.0 | 103.1 | 96.7 | −7.5 | 127.1 | 138.8 | 10.8 |
| E–W-washed | | 136.0 | 151.8 | 24.5 | 102.5 | 95.8 | −7.5 | 129.0 | 139.3 | 9.7 |
| 50E–W-washed | | 124.1 | 152.7 | 29.1 | 100.8 | 94.2 | −13.5 | 120.7 | 135.9 | 16.8 |

The samples were prepared according to method OP with 16 h complexation time. W, E, and 50E denote the use of water, ethanol, and 50% v/v aqueous ethanol, respectively.

higher $\Delta H$ of the W-washed complex is likely due to the more crystalline structure compared to the unwashed complex.

Regarding the use of ethanol, the resulted amylose–PTHF650 complexes show no melting endotherm of PTHF independent of the sequence of the use of water and ethanol for washing. These complexes show a high $t_m$ (152–153 °C) on the first heating compared to the $t_m$ of the unwashed and W-washed complexes (134 °C). However, the resulted endothermic peak on the first heating became broad for the complexes that were rewashed using cold water [E–W-complexes, onset temperature ($t_o$) at 136 °C] and even broader for the one that was washed using less ethanol with subsequent cold water washing (50E–W-complexes, $t_o$ at 124 °C).

The E–W- and the 50E–W-complexes show a higher $\Delta H_m$ on the first heating (29 J g$^{-1}$) compared to the other ones. However, the low $t_o$ of the 50E–W-complex (124.1 °C) closely resembles the $t_o$ of the W-washed complex (125.7 °C). In the case of 50% v/v of ethanol, the loosely bound PTHF was not dissolved as effective as it was in 100% ethanol. As a consequence, the thermal behavior of the resulted 50E–W-complex is a combination of water- and ethanol-washed amylose–PTHF complexes: high $t_m$ and high $\Delta H_m$ with a broad endothermic peak. Furthermore, by comparing the $\Delta H_c$ of the 50E–W-complex (around −14 J g$^{-1}$) with the E- and E–W-complexes ($\Delta H_c$ around −8 J g$^{-1}$), there is an indication that only a small amount of the PTHF is removed for the complex that was washed by 50% v/v ethanol. This is also supported by the fact that the $\Delta H_m$ on the second heating for the 50E–W-complex (17 J g$^{-1}$) is also higher than the E- and E–W-complexes (10 and 11 J g$^{-1}$).

Additional measurements by applying a 1h isothermic treatment at 85 °C were also performed on the amylose–PTHF650 complexes. However, even after being equilibrated during cooling, the $\Delta H_m$ for the washed complexes on the second heating is lower than the first heating. In the case of E- and E–W-complexes, the similar $\Delta H_m$ on the second heating (12–13 J g$^{-1}$) indicates that the high $\Delta H_m$ on the first heating (25–27 J g$^{-1}$) is associated with the quality rather than the degree of crystallinity.

### 3.1. XRD Measurements on Amylose–PTHF650 Complexes

As shown in the X-ray diffractograms (Figure 2), PTHF650 has a main diffraction ($2\theta$) at 19.9° and an additional peak at 24.4°. As for the amylose–PTHF650 complexes, beside the main diffraction peaks ($2\theta$) at 13.0°–13.3° and 19.8°–20.0°, more peaks are detected compared to the amylose–PTHF1000 complexes. These additional peaks, especially at the $2\theta$ of 17.3°, 18.6°, 21.4°, and 22.5° are clearer observable for the E-washed complex. Furthermore, the E-washed complex shows more similarity to starch-decanal complexes by having a small diffraction at 7.5° that corresponds to a $d$-spacing of 1.18 nm (plane 110, see Supporting Information, Table S1).

The peak at 22.5° ($d = 0.39$ nm) is the least sharp for the E–W-washed amylose–PTHF650 complex (Figure 2e). The peak at 21.4° ($d = 0.41$ nm) is sharper for the complexes that were washed with 100% ethanol (E- and E–W-washed complexes; Figure 2). This peak fits well with the diffractions of amylose–*n*-butanol/*n*-pentanol complexes (from plane 450).[4] This means that the amylose–PTHF650 complexes adopt a $V_{6II}$-amylose structure that provides a space in between the amylose helices to accommodate the PTHF650. This furthermore means that ethanol washing did not change the dimension of the crystal structure of the amylose–PTHF650 complexes.

Based on the possibility that some of the included PTHFs are located in between the amylose helices, the resulted crystals probably adapt as $V_6$-amylose with a

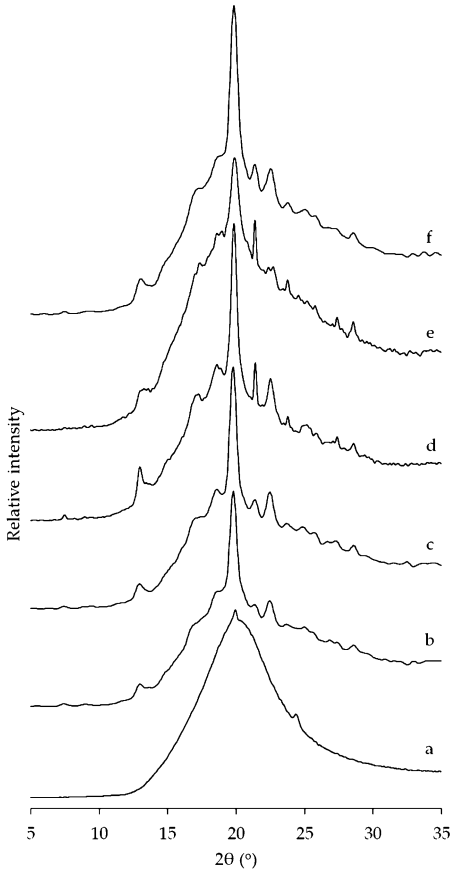


*Figure 2.* X-ray diffractograms of a) PTHF650 and b) inclusion complexes between amylose and PTHF650 that were unwashed and freeze-dried, c) W-washed and freeze-dried, d) E-washed and air-dried, e) E–W-washed and freeze-dried, f) 50E–W-washed and freeze-dried. W and E denote water and ethanol.

larger dimension, such as for the complex between amylose and *n*-butanol or *n*-pentanol.[4] The crystal structure of amylose–*n*-butanol/*n*-pentanol complexes was reported as a six-fold amylose helix with an orthorhombic crystal having a dimension of $a = 2.74$ nm, $b = 2.65$ nm, and $c = 0.8$ nm.[4] Using those cell parameters, the peak at 21.4° ($d = 0.41$ nm) is associated with the diffraction plane with the *hkl* value of 530 (see Supporting Information Table S1). As for the peak at 22.5° ($d = 0.39$ nm), besides fitting to the diffraction of plane 311 of amylose–fatty acids complexes, it also fits to the diffraction of plane 202 of the amylose–alcohol complexes. Another peak that also matches with the amylose–alcohol complexes is the diffraction at $2\theta$ of 18.7°–19.0° ($d = 0.47$ nm, plane 530).

Another guest induced V-amylose to consider is the complex between amylose and α-naphthol. The resulted V-amylose was reported as an eight-fold helix in which the α-naphthol resided inside and in between the helices and crystallized as a tetragonal packed structure with a cell parameter of $a = b = 2.2844$ nm and $c = 0.7806$ nm.[40] Using these cell parameters, the diffraction peak ($2\theta$) at 16.7°–16.8° that was observed for the unwashed and W-washed amylose–PTHF650 complexes correspond to a $d = 0.53$ nm that results from the diffraction of plane 131. However, since the diffracted peak at 16.7°–16.8° is generally observed as a shoulder rather than a real peak, it is proposed that the resulted amylose–PTHF complexes described here are likely to adopt a V-amylose conformation with six glucose residues per helix turn ($V_6$-amylose) rather than a $V_8$-amylose conformation. Furthermore, there is also the possibility that the shoulder-shaped peak at 16.7°–16.8° is from amylose itself as the amorphous part of amylose has a broad diffraction pattern.

The possible amylose peak at around 16.7°–17.3°can be from retrograded amylose (either A- or B-amylose). However, the intensity of the diffractions is small and the correlating DSC results did not show melting peaks of (free) uncomplexed amylose which should appear upon heating at around 150 °C. In addition, the retrogradation peak of the amylose which should appear upon cooling at around 50–70 °C was not observed as the amylose formed complexes with PTHF. In this case, the observed diffraction peak of the amylose is likely from the small rupture within the amylose helices.

The effects of the amount of water on the resulting crystal structure of amylose–PTHF650 complexes.

The amylose–PTHF complexes consist of amylose as host molecules and PTHF as guest molecules. The presence of many hydroxyl groups in the amylose chain attracts water molecules by forming hydrogen bonds. Therefore, besides consisting of amylose and PTHF, the amylose–PTHF complex also contains water as its building molecules. In this case, the water content of the air-dried product is estimated around 10% w/w while the freeze-dried products contain around 3% w/w water.

To investigate the effect of the amount of water on the resulting products, additional XRD measurements without additional moistening were performed. As shown in Figure 3, when the amylose–PTHF650 complexes were measured without being moistened over $K_2CO_3$, the diffraction peaks showed different patterns compared to Figure 2 (moistened over $K_2CO_3$ results in 40% relative humidity, Rh). Without moistening to 40% Rh, hence less water content, the peak at $2\theta$ of 13.1°–13.6° ($d$-spacing of 0.65–0.68 nm) became more pronounced (Figure 3). As the difference between Figure 2 and 3 was the preparation of the samples just before the XRD measurements, the peak at $2\theta$ of 13.1°–13.6° probably correlates to the water content. The increased sharpness of this peak suggests that less water content leads to a more crystalline amylose–PTHF complex. Interestingly, the diffraction peak of the unwashed amylose–PTHF650 complex at $2\theta$ of 20.7° has a shoulder peak at 19.9°. The peak appears at 19.9°/20.0°

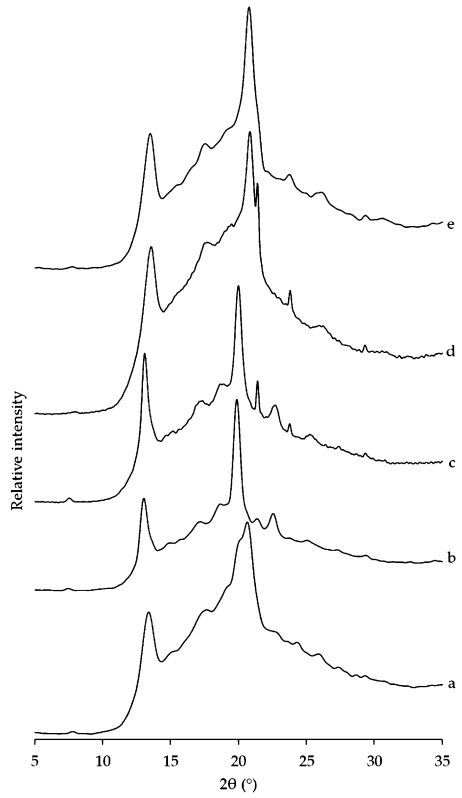


*Figure 3.* X-ray diffractograms of inclusion complexes between amylose and PTHF650 that were a) unwashed and freeze-dried, b) W-washed and freeze-dried, c) E-washed and air-dried, d) E–W-washed and freeze-dried, e) 50E–W-washed and freeze-dried. The samples were directly measured, without moistening over $K_2CO_3$.

(*d*-spacing of 0.44–0.45 nm) for the W- and E-washed products, and at 20.8° (*d*-spacing of 0.43 nm) for the E–W- and 50E–W-washed products. The peak also correlates to the amount of water, as the peak appears at 2$\theta$ of 19.8°–19.9° for all products with 40% Rh (Figure 2) and no significant differences were observed for the other diffraction peaks.

The fact that the W- and the E-washed products diffracted at similar 2$\theta$ (19.9°–20.0°) shows that the two products accommodate a similar number of water molecules in the resulted crystals, despite being dried in different ways. This means that even though the E-washed complex has no PTHF in between the amylose helices, the position of the water molecules after being washed with water stayed the same. In this case, the ethanol washing only affects the included PTHFs and did not influence the included water molecules. In addition, rather than fitting to the crystal structure of amylose–fatty acid complexes,[9] the corresponding *d*-spacing of 0.43 nm fits closely to the diffraction of plane 521 of amylose–*n*-butanol/*n*-pentanol complexes.[4]

A similar water content is present in the E–W- and 50E–W-washed amylose–PTHF650 complexes as both products diffracted at 2$\theta$ of 20.8°. This indicates that after ethanol washing (both 50 and 100% EtOH), the PTHF chains that reside in between the helices were washed away, thus leaving some voids in the crystals. When water was introduced to result in E–W- and 50E–W-washed products, the water molecules penetrated the crystals and filled all or some voids that were left by the washed PTHFs. The interstitial matrices that had been occupied by water molecules thus diffracted at different angle (2$\theta$ at 20.8°). The diffraction area between 15 and 21° of the E–W- and 50E–W-washed complexes also closely resemble the unwashed complex. This shows that in the case of the unwashed products, there is inhomogeneity of water content of the resulted complex. Some amylose helices probably have sufficient water molecules as the E–W- and 50E–W-washed complexes, while the rest have less water molecules similar to the W- and E-washed complexes. This is due to the insufficient number of PTHF chains that were used for complexation to fill in all the available interstitial matrices in the resulted amylose–PTHF650 unwashed complexes.

### 3.2. Water and Ethanol as Washing Solvents for Amylose–PTHF1000 Complexes

Ethanol washing was also performed on amylose–PTHF1000 complexes. In this study, three samples with different complexation times were used and purified with the same purification method. As shown in Table 2, in the

*Table 2.* DSC data of ethanol-washed inclusion complexes between amylose and PTHF1000.

| Inclusion complexes | First heating scan | | | First cooling scan | | | Second heating scan | | |
|---|---|---|---|---|---|---|---|---|---|
| | Onset [°C] | Peak [°C] | $\Delta H$ [J g$^{-1}$] | Onset [°C] | Peak [°C] | $\Delta H$ [J g$^{-1}$] | Onset [°C] | Peak [°C] | $\Delta H$ [J g$^{-1}$] |
| 0 h-E-washed | 116.5 | 136.0 | 40.4 | 98.1 | 91.5 | −15.5 | 118.6 | 135.5 | 20.0 |
| 1 h-E-washed | 131.5 | 148.5 | 38.0 | 104.4 | 95.2 | −13.5 | 123.3 | 139.2 | 15.4 |
| 16 h-E-washed | 138.9 | 148.9 | n.c.[a)] | 102.2 | 93.2 | −13.9 | 121.7 | 139.2 | 17.6 |

[a)]n.c. = Not calculated. The 0 h-complexes were prepared by method IS, while the 1 h- and 16 h-complexes were prepared by method OP. E denotes ethanol.

first heating scan the $t_m$ of the ethanol-washed (E-washed) amylose–PTHF1000 complex that was prepared by method IS for 0 h-mixing time ($t_m$ 136 °C) is lower compared to the 1 h- and 16 h-E-washed amylose–PTHF1000 complexes ($t_m$ 149 °C). This indicates that regardless of the purification method, longer mixing times result in more crystalline complexes. The corresponding $\Delta H_m$ for 0 h- and 1 h-E-washed amylose–PTHF1000 complexes show similar values (38–40 J g$^{-1}$) which means that the amount of the complexes for both complexes is similar. In addition, the corresponding $\Delta H_c$ (between –14 and –16 J g$^{-1}$) and the $\Delta H_m$ in the second heating (15–20 J g$^{-1}$) are also similar. This shows that for a similar purification method, complexation time gives no influence to the number of the resulting complexes. The number of the complexes as well as the quality of the crystallinity likely influences the high enthalpy values of the E-washed products. In addition, the drying methods which involve the use of freeze drying (for W-washed products) and conventional air drying (for E-washed products) seem to give no significant effects on the properties of the resulted complexes.

There are three kinds of PTHFs that can attribute to the endothermic of PTHF: fully uncomplexed (free) PTHF, partly complexed PTHF and PTHF residing in between the amylose helices. The three PTHFs will show a similar $t_m$. This $t_m$ of PTHF, which was present in the unwashed and water-washed (W-washed) complexes, is not visible in the products that were washed by ethanol. For the 0 h-E-washed complex, a $\Delta H_m$ (40 J g$^{-1}$) in the first scan was observed. This enthalpy is higher compared to the $\Delta H_m$ values of the 0h-unwashed complex (23 J g$^{-1}$) and the 0 h-W-washed complex (30 J g$^{-1}$). In this case, it is possible that the ethanol reduced the amount of the complexes. This is confirmed by the visible amylose retrogradation that was observed for the E-washed complexes. Even though the retrogaradation is smaller compared to the unwashed products, it shows that some PTHFs that resided inside the amylose cavity were taken away by the ethanol. This was not observed for the water-washed products.

As no visible melting of PTHF was observed ethanol washed away all PTHF chains. This shows that as the PTHFs residing in between the amylose helices are loosely bound, ethanol as a good solvent for PTHF removed the PTHF chains easily. Furthermore, the $\Delta H_m$'s on the second heating for the 0 h-, 1 h-, and 16 h-complexes that were ethanol-washed (15–20 J g$^{-1}$) were always lower than the corresponding $\Delta H_m$ on the second heating of the water-washed complexes (23–30 J g$^{-1}$). The lower $\Delta H_m$'s on the second heating relate with the quality of the crystallinity of the ethanol-washed complexes. The $\Delta H_m$ of the first heating of the ethanol-washed products relates to less crystals but with higher crystallinity. Thus, the detected $\Delta H_c$ of the ethanol-washed complexes during cooling is lower which leads to lower $\Delta H_m$ on the second heating compared to the corresponding water-washed complexes. The schematic representation of the ethanol washing is depicted in Figure 4.

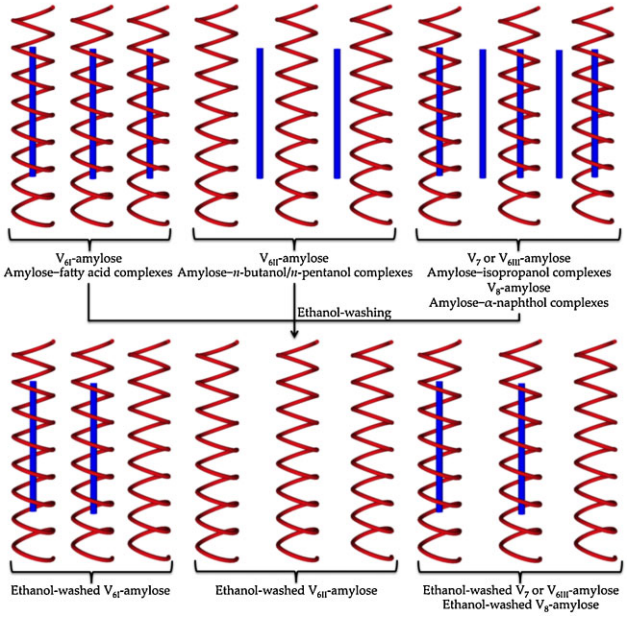


*Figure 4.* Schematic representation of ethanol-washing of the complexes between amylose (red) and PTHF (blue) assuming that three kinds of V-amylose are possibly adopted by amylose–PTHF complexes.

An isothermic for 1 h at 85 °C was also performed on the 1 h-E-washed amylose–PTHF1000 complexes. The resulted $\Delta H_m$ on the second heating is increased (22.7 J g$^{-1}$) compared to the one without additional isotherm ($\Delta H_m$ on the second heating is around 15 J g$^{-1}$). However, even after an isothermic treatment, the $\Delta H_m$ on the second heating of the ethanol washed complex is lower compared to the water-washed complexes ($\Delta H_m$ of 1 h-W-washed complex after additional isotherm is around 27 J g$^{-1}$). This trend shows that even though the ethanol helps arranging the complexes into a more crystalline structure, it also takes out some PTHF thereby reducing the amount of the complexes.

### 3.3. XRD Measurements of Amylose–PTHF1000 Complexes

As shown in Figure 5, the diffraction pattern of the 0 h-E-washed amylose–PTHF1000 complex show only one diffraction peak (2$\theta$) at 20°, with a shoulder at 12°–13°. This means that for an immediate complexation, the guest PTHF in the resulting complexes occupies the inside cavity of the amylose. In addition, the peak at 20.3° for the 0 h-E-washed complex appeared sharp showing high crystallinity. The diffraction peak at around 20° becomes sharper for complexes that were prepared with longer reaction time (1 and 16 h). The peak at around 13° also becomes sharper and

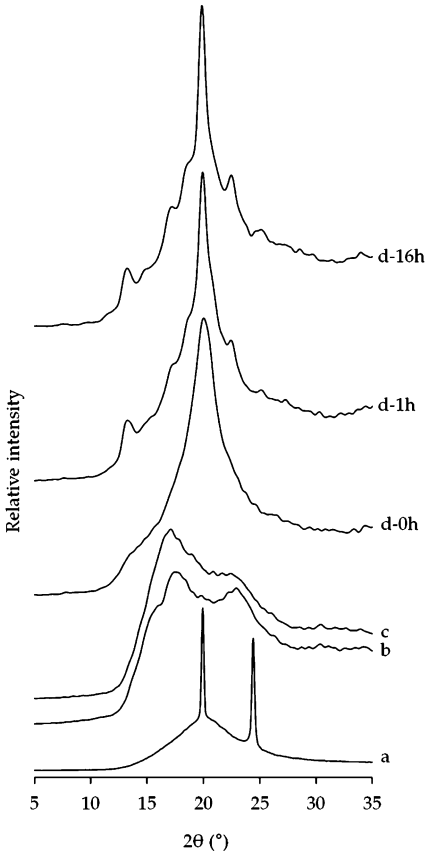


*Figure 5.* X-ray diffractrograms of a) PTHF1000, b) amylose, c) freeze-dried amylose after heating, and d) inclusion complexes between amylose and PTHF1000 that were ethanol-washed.

more additional diffractions were observed for 1 h- and 16 h-E-washed amylose–PTHF1000 complexes. This shows that despite being washed with ethanol, longer complexation time resulted in more crystalline complexes. As the DSC data of the 0 h-, 1 h-, and 16 h-E-washed amylose–PTHF1000 complexes showed no visible endothermic peak of PTHF, this means that free PTHF and the PTHF that resides in between the helices were washed away.

Even though the XRD data showed no apparent amylose peaks for the E-washed products, the corresponding DSC data of the products showed visible amylose retrogradation. This means that the retrograded amylose detected by the DSC is from the amorphous part of the crystal of the complexes. This results from amylose chains that just partially formed inclusion complexes with PTHF.

The main diffraction peaks of the E-washed amylose–PTHF1000 complexes are observed at 12.9°–13.1° and 19.7°–19.8°. By using the indexes of the orthorhombic unit cell of amylose–fatty acids complexes reported by Zobel et al. ($a = 13.6$, $b = 23.7$, $c = 8.1$ Å), these diffractions correspond to the reflections of plane 200 and 310, respectively (see Supporting Information, Table S2). Similar to the unwashed and the W-washed amylose–PTHF1000 complexes, the diffractions fit with the amylose–fatty acids complex ($V_{6I}$-amylose) with a diffraction at around 22.1° which can also fit the $V_{6II}$-amylose. As the actual structure of amylose–PTHF complex is not yet known, the presence of the $V_{6I}$- and the $V_{6II}$-amylose remains debatable. However, for the E-washed complexes, the DSC and the XRD data demonstrated that the guest PTHF resides inside the cavity of the amylose helices.

### 3.4. Solvent Stability of Amylose–PTHF Complexes

Solvents with a good ability to dissolve PTHF were used to wash the 1 h-ethanol-washed (1 h-E-washed) amylose–PTHF1000 inclusion complex. The complex was chosen because it contains no endothermic peak of PTHF during heating in the DSC. Therefore, the resulted effects caused by the solvents will only affect the complexes. The enthalpy data of the complexes are shown in Table 3, in which the endothermic enthalpy ($\Delta H_m$) of the first heating scan was estimated roughly due to baseline effects. The onset melting temperatures ($t_o$) of the first heating of the complexes rewashed by THF, $CHCl_3$, and $CH_2Cl_2$ are shifted towards higher temperatures ($t_m = 137$–$147$ °C). The $\Delta H_m$'s are also higher, in the range of 90–115 J g$^{-1}$, compared to the original complex ($t_o = 129$ °C, $\Delta H_m \approx 80$ J g$^{-1}$). The narrower endothermic peaks of the rewashed complexes indicate that the rewashed complexes are more crystalline than the original complex. However, the corresponding exothermic enthalpy for the rewashed complexes are slightly lower (between −12 and −14 J g$^{-1}$) and consequently lead to a slightly larger enthalpy of the amylose retrogradation (between −4 and −6 J g$^{-1}$). Furthermore, even though the $\Delta H_m$ during the second heating of the original complex (26 J g$^{-1}$) is already lower than the corresponding $\Delta H_m$ during the first heating, the corresponding $\Delta H_m$ of the rewashed complexes are even lower (17–22 J g$^{-1}$). This indicates that after rewashing, the amount of complexes in the rewashed products is decreased. This trend shows that the observed endothermic enthalpies likely correlate more with the quality of the crystallinity rather than the quantity of the complexes as the cooling scan shows that the numbers of the complexes are reduced. In this case, the solvents washed out some included PTHF, thus favored more amylose retrogradation.

The way the solvents promote better crystallinity while washing out some included PTHFs is associated with the possibility that the included PTHFs are not equally arranged in the crystal lattice. Consequently, the loosely bound PTHFs which presumably account for less crystallinity, were easier to dissociate from the amylose helices upon the solvation of the complexes. The loss of these PTHF chains promoted better arrangement in the crystal packing which resulted in very high endothermic enthalpies during the

*Table 3.* DSC data of the rewashed inclusion complexes between amylose and PTHF1000.

| | First heating scan | | | First cooling scan | | | | | | Second heating scan | | |
|---|---|---|---|---|---|---|---|---|---|---|---|---|
| | Inclusion complexes | | | Inclusion complexes | | | Amylose retrogradation | | | Inclusion complexes | | |
| Inclusion complexes | Onset [°C] | Peak [°C] | $\Delta H$[a)] [J g$^{-1}$] | Onset [°C] | Peak [°C] | $\Delta H$ [J g$^{-1}$] | Onset [°C] | Peak [°C] | $\Delta H$ [J g$^{-1}$] | Onset [°C] | Peak [°C] | $\Delta H$ [J g$^{-1}$] |
| Original | 129.1 | 149.6 | 79 | 90.8 | 86.0 | −14.6 | 52.3 | 38.0 | −2.9 | 99.1 | 124.7 | 26.1 |
| Rewashed | | | | | | | | | | | | |
| THF | 147.0 | 155.4 | 89 | 91.0 | 86.5 | −13.8 | 53.5 | 41.0 | −4.5 | 110.1 | 125.7 | 16.9 |
| $CHCl_3$ | 136.6 | 151.4 | 114 | 91.6 | 87.0 | −12.4 | 55.8 | 43.5 | −5.3 | 102.7 | 124.0 | 17.7 |
| $CH_2Cl_2$ | 138.6 | 153.1 | 103 | 90.7 | 86.7 | −12.8 | 55.6 | 45.7 | −5.9 | 106.2 | 124.0 | 21.8 |
| THF/EtOH | 141.6 | 155.1 | 60 | 90.4 | 85.2 | −9.3 | 57.2 | 48.3 | −9.8 | 105.7 | 125.7 | 8.8 |

[a)]The values were roughly determined. The samples were heated from 1 to 170 °C, cooled from 170 to 1 °C, and heated again from 1 to 170 °C at 10 °C min$^{-1}$. THF/EtOH was used as 1:1 v/v.

first heating. As the crystals gained more mobility, some part of the amylose chains that were occupied with the loosely bound PTHF became able to have intermolecular interaction, which resulted in more retrogradation.

However, opposite effects on the crystallinity were observed for the complexes suspended in THF/EtOH. Despite having a high onset temperature (142 °C), the $\Delta H_m$ on the first heating (60 J g$^{-1}$) is lower than the original complex (79 J g$^{-1}$). The retrogradation of the amylose in this complex is also three times higher ($\Delta H_c \approx -10$ J g$^{-1}$) and the $\Delta H_m$ on the second heating (9 J g$^{-1}$) is around three times less compared to the original product (26 J g$^{-1}$). This shows that even though the crystallinity of the complex is higher than the original one, the number of the complexes is less even in comparison with the other rewashed complexes. In this case, the use of THF/EtOH resulted in the lowest crystallinity with the highest loss of the guest PTHF. In comparison with the other solvents, the order of this solvent effect is THF/EtOH > THF > $CHCl_3$ > $CH_2Cl_2$.

The fact that THF/EtOH dissolved more PTHF and reduced the crystallinity of the amylose–PTHF complexes is due to its ability to form hydrogen bonds with amylose. As THF, $CHCl_3$, $CH_2Cl_2$ cannot form hydrogen bonds with amylose, the loss of the included PTHF is thus based on the solvation only. In contrast to this, ethanol is able to interact better with amylose and thereby facilitates the solvation process. In addition, ethanol is also known as a precipitant that can induce the formation of $V_6$-amylose without being included in the amylose chain.[41] Even though the resulted $V_6$-amylose crystal contains only amylose and water and involves no ethanol molecules, there is a probability that ethanol is included in the amylose helices in the first stage of the $V_6$-amylose formation.[41] In the case of the amylose–PTHF1000 complex, as the ethanol formed hydrogen bonding and changed the arrangement of the amylose helices, an equilibrium or an exchange of the guest molecules between PTHF and ethanol was achieved. As the amount of ethanol is larger than the amount of PTHF, the exchange process thus became more favorable. Due to this exchange, even though the ethanol still maintained the $V_6$-amylose form in the amylose–PTHF complexes, the amylose was then more prone to retrogradation, because there were less guest molecules inside its helices. This is confirmed by the larger amylose retrogradation and less $\Delta H_m$ of the complexes shown in Table 3.

The diffractograms of the rewashed complexes are depicted in Figure 6. Due to amylose retrogradation, the

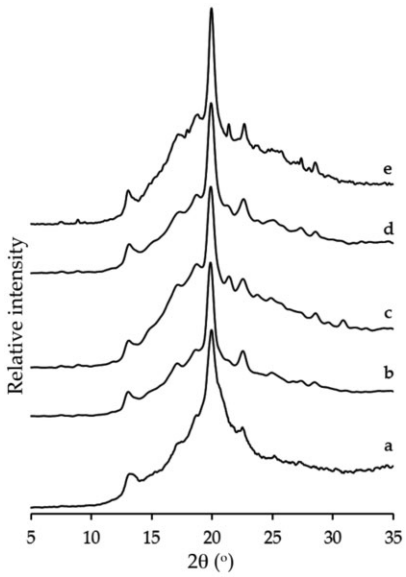


*Figure 6.* X-ray diffractograms of a) the 1 h-E-washed amylose-PTHF1000 complexes and b) the corresponding products that were rewashed with THF, c) $CHCl_3$, d) $CH_2Cl_2$, and e) THF/EtOH.

diffraction of amylose was observed at 17.1°–17.3°. The rewashed amylose–PTHF1000 complexes have three main diffraction peaks that resemble an orthorhombic crystal of amylose–fatty acid: $2\theta$ at 13.3°, 19.9°, and 22.6°. The peaks correlate with the diffractions from the planes 200, 310, and 311, respectively (see Supporting Information Table 3). As described before, some of these peaks especially the strong diffraction ($2\theta$) at 21.4° that corresponds to the plane 441, represent the diffraction of an orthorhombic crystal similar to amylose–*n*-butanol/*n*-pentanol.[4]

The observed diffractions of the rewashed amylose–PTHF1000 complexes are not all identified. However, there are also peaks with low intensity that can be identified by fitting them with the calculation of the amylose–isopropanol/acetone complexes having a cell parameter of $a = 28.26$ Å, $b = 29.30$ Å, and $c = 8.01$ Å (see Supporting Information, Table S3).[32] The location of the isopropanol or acetone in the resulting crystal was reported to reside in between the helices and the crystal shrunk and converted to $V_h$-amylose upon desolvation by methanol.[32] As for the rewashed amylose–PTHF1000 complexes described here, the main diffractions that correspond to $V_h$-amylose remains unchanged which means that the guest PTHFs are still in the cavity of the amylose.

For the THF/EtOH-rewashed complex, the diffraction peak at 21.4° tend to appear strongly compared to the other rewashed amylose–PTHF1000 complexes. As the diffraction peak at 21.4° fit with the calculation of the amylose–*n*-butanol/*n*-pentanol complexes, it indicates that the peak correlates to the PTHF chains that are located in between the amylose helices, either partly or as a whole. It has been reported for amylose-fatty acid complexes that entanglement might occur, in which the tail of the fatty acid is included in two different helix segments.[42] In this case, the including helix segments can be either from the same or from different amylose helices. As in the case of the THF/EtOH-rewashed amylose–PTHF1000 complexes, the ethanol shoved the position of the included PTHF inside the helix cavity of the amylose, thus resulting in a bigger part of PTHF that is located in between the helices compared to the original product. Nevertheless, this tendency supports the possibility that PTHF chains are included inside and in between the amylose helices.

### 3.5. Morphology of Amylose–PTHF Complexes

16 h-E-washed amylose–PTHF650 and amylose–PTHF1000 complexes were used as these PTHFs have good complexing abilities with amylose. In addition the DSC did not show any trace of PTHF, neither amylose retrogradation, thereby avoiding the confusion from crystals that come from free amylose or free PTHF.

The morphologies of the amylose–PTHF650/PTHF1000 complexes that were prepared by slow recrystallization are shown in Figure 7. The resulting crystals generally assembled as round shaped crystals with concave centers.

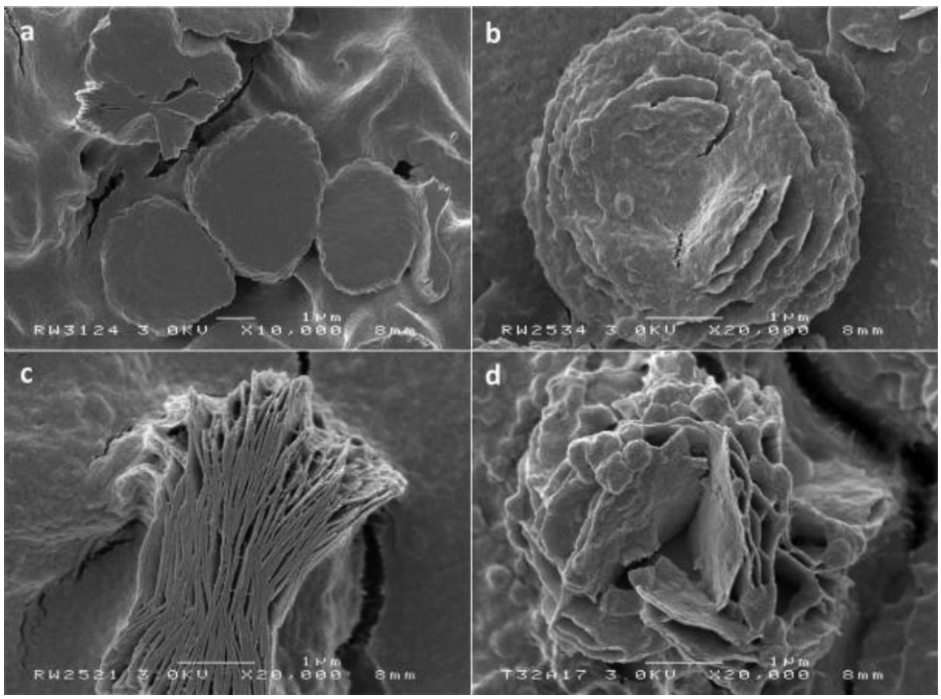


*Figure 7.* SEM images of amylose–PTHF complexes. The complexes were recrystallized by slow cooling at 60 °C without annealing (a: amylose–PTHF650), at room temperature with subsequent annealing at 40 °C for 2 h (b,c: amylose–PTHF650), and 30 min (d: amylose–PTHF1000 complexes).

Most of the crystals are more clearly distinguished from the matrix for the ones that were additionally annealed at 40 °C compared to unannealed crystals. Besides swollen-like round crystals having concave centers, there are also some round crystals with a flat surface. The shape of the swollen-like round crystals is clearly visible and distinctive from the matrix (see Supporting Information, Figure S1). These crystals were observed to have a diameter ranging between 4 and 6 μm. As for the resulted concave centers, this is likely due to the round lamellae that stacked vertically on top of one another with an outward growth direction. Based on the spherulitic intermediate shown in Figure 7c, the depth of the round crystals is around 2 μm, while the thickness of the stacked lamellae layers is around 50 nm. Some lamellae grew in a bent direction forming a flower-like structure as shown in (Figure 7d).

Although most of the matrix was seen as a smooth area, some half-growth lamellae were observed from the matrix as well. This shows that in the first stage of the crystallization, the crystal grew as a single lamellae layer which then induced another growth of the lamellae. Here, chain folding of the PTHF-containing amylose likely happened and resulted in a supramolecular structure. As for the flower-like structures that were also observed for amylose–PTHF1000 complexes it shows that the constructing lamellae likely grew from the same nucleus. In addition, as most of the resulted structures are not a single crystal, this indicates that the nucleation process was heterogeneous.[36] The presence of the matrix itself indicates that the amorphous part in the complex is unavoidable due to the long amylose chain.

The flat surface structures of the amylose–PTHF650 complexes were also seen to form aggregates with a larger surface area with some lamellae layers which were observed to cross one another (Supporting Information, Figure S2a). There are also needle-like structures (Supporting Information, Figure S2b3), which is in agreement with the previously reported observation based on polarized light microscopy.[24]

Most of the resulted crystals of the amylose–PTHF1000 complexes prepared by recrystallization with cooling at room temperature have a round shape with a flat surface (Supporting Information, Figure S3a). In contrast, the recrystallization with cooling at 85 °C resulted in crystals with a fringed lamella (Supporting Information, Figure S3b).

To avoid aggregation of the amylose–PTHF1000 complexes, the recrystallization was performed with a low concentration of the complex (1 g $L^{-1}$). The recrystallization by slow cooling at room temperature resulted in platelets (Supporting Information, Figure S3a1). The diameter of a full flat surface flake ranges between 4 and 8 μm. There are also some flakes that appeared half-grown and resembled some lamellae which were vertically arranged. These structures closely follow the growth mechanism of a spherulitic superstructure proposed by López and Wilkes in which the radial growth of the lamellae resulted in sheaf-like intermediates.[43] With the same crystallization treatment, there are also some lamellae that seemed to grow side-by-side, yielding a flower-like crystal (Figure 7d). This shape was also observed for inclusion complexes between amylose and α-naphthol reported by Putaux et al.[36] However, the resulted amylose–PTHF1000 crystals were clearly surrounded by some amorphous matrix area. This indicates that a part of the complex was amorphous.

Because amylose with long chains ($M_v \approx 200$ kg $mol^{-1}$, $\overline{DP}_n$ around 1235) were used, the possibility of having an amorphous part due to the guest free location or a small helix rupture seems to be high.[6] In addition, when the sample was kept under the vacuum for 3 min, the resulted crack within the amorphous matrix revealed the presence of some tubular-shaped forms in the range of 0.2–0.5 μm (Supporting Information, Figure S3a2). As a $V_6$-amylose has a *c* parameter of 0.81 nm,[9] an amylose with $\overline{DP}_n$ 1235 thus contains around 206 helix turns, making a total length of around 0.17 μm per straight amylose chain. Based on this calculation, the tubular shape is a small part of the crystal, which grows further as a lamella.

Recrystallization at 85 °C of the amylose–PTHF1000 complexes resulted in structures that arranged as some layered platelets. This indicates that the resulting lamellae probably induced the growth of another lamellae and resulted in a stacked layer. These stacked layers tend to aggregate randomly thereby generally observed with different length. When the growing lamellae stacked side-by-side rather than on top of one another, the thinner layer was barely distinguished from the matrix (Supporting Information Figure S3b1). The sheaf-like structures, which accounted as the intermediate of the radial spherulitic growth of the lamellae, were seen as vertically flipped lamellae stacks (Supporting Information Figure S3b2). The thickness of the lamellae ranges between 20 and 120 nm.

Based on the above investigation, the variation on the concentration, cooling temperature of the recrystallization, and additional annealing of the amylose–PTHF650/PTHF1000 complexes generally resulted in a similar assembly. Most of the structures were round crystals having a diameter between 4 and 8 μm with 2 μm in depth, with the constructing lamella having a thickness of 20–50 nm. The depth of the round crystals likely correlates to the diameter of the flat-surfaced crystals of the spherulitic round structures with a diameter of 2–4 μm. The similarity shows that regardless the length of the guest PTHF, the amylose–PTHF complexes tend to aggregate in a similar manner that resulted in similar structures. To get a single crystal, synthetic amylose with a perfectly linear chain and $\overline{DP}_n$ that corresponds closely to the length of one or two

PTHFs to avoid chain folding seems to be preferable. In this case, a single crystal of the amylose–PTHF is expected to be a round shaped lamella.

Based on an assumption that the amylose–PTHF complexes adopt a $V_6$-amylose with a *c* parameter of 0.81 nm,[9] the lamella thickness of 20–50 nm corresponds with 25–63 straight helix turns. This indicates that for a whole chain of potato amylose ($M_v \approx 200\ kg\ mol^{-1}$; $\overline{DP}_n$ 1235 contains around 206 helix turns), around 12–31% of the amylose helix turns construct the crystalline lamella. This means that around 69–88% of the amylose helix turns form amorphous networks.

Additionally, based on a calculation that a repeating unit of PTHF is ca. 6.0 Å,[15] PTHF650 corresponds with 5.42 nm in length and PTHF1000 is around 8.4 nm in length. In this case, one straight helix of potato amylose can accommodate up to 31 chains of PTHF650 and 20 chains of PTHF1000. By assuming that the guest PTHF inside the amylose helices is packed as a vertically straight organization, a 20–50 nm of lamella thickness also corresponds with around 3–9 chains of PTHF650 and around 2–6 chains of PTHF1000.

The XRD data of the 16 h-E-washed amylose–PTHF650/PTHF1000 complexes described (Figures 2,5) showed a more crystalline structure compared to other complexes that were prepared with shorter mixing time. In this case, it is expected that the resulting morphology shows a distinctive structure of crystalline lamellae with less amorphous area. However, the observed morphologies by SEM showed that the amorphous layers cannot be avoided. Furthermore, the XRD and the DSC data of the 16 h-E-washed complexes showed no uncomplexed amylose and free PTHF which eliminates the possibility of having amorphous area due to a fully uncomplexed amylose. This means that the amorphous part that was observed here is constructed of amylose–PTHF complexes. This indicates that the general morphology of amylose–PTHF inclusion complexes is lamellar which consists of alternating crystalline and amorphous layers.

## 4. Conclusion

Upon washing amylose–PTHF complexes were stable showing an increase in crystallinity. Furthermore, the use of water in different sequences with the main washing solvent resulted in a slightly different structure. In this case, even though the definite crystal structure of amylose–PTHF inclusion complexes is not known yet, the resulted crystal structures of amylose–PTHF complexes seem to be affected by the amount of the included water molecules. The stability of the complexes was still retained after additional rewashing process of the complexes in some organic solvents, except in precipitants that can induce formation of V-amylose, such as ethanol. With XRD data it was proven that the main diffractions of the rewashed amylose–PTHF complexes correspond to the diffractions of an orthorhombic crystal of amylose–fatty acid complexes. Some diffraction correlated to the cell parameters of the amylose–*n*-butanol/*n*-pentanol and amylose–isopropanol/acetone complexes. These diffractions support the possibility that the structure of the amylose–PTHF complexes is a six-fold V-amylose helix in the form of a mixture or an intermediate of $V_{6I}$- and $V_{6II}$-amylose. In addition, SEM analysis shows that amylose–PTHF complexes assembled as around spherulitic supramolecular structures which were constructed by vertically stacked round lamellae.

Acknowledgements: The authors thank the group of Solid State Materials for Electronics (Zernike Institute for Advanced Materials, University of Groningen, The Netherlands) for access to the X-ray Diffraction spectrometer and Evgeny Polushkin for the SEM images. The research was financed by a Bernoulli Scholarship from the Zernike Institute for Advanced Materials and by a VIDI innovational research grant from the Netherlands Organisation for Scientific Research (NWO).

Received: April 4, 2013; Revised: July 17, 2013; Published online: August 28, 2013; DOI: 10.1002/mabi.201300174

Keywords: amylose; inclusion chemistry; mixing; polytetrahydrofuran; solvent responsive

[1] F. L. Bates, D. French, R. E. Rundle, *J. Am. Chem. Soc.* **1943**, *65*, 142.
[2] S. Immel, F. W. Lichtenthaler, *Starch/Stärke* **2000**, *52*, 1.
[3] M. A. Whittam, P. D. Orford, S. G. Ring, S. A. Clark, M. L. Parker, P. Cairns, M. J. Miles, *Int. J. Biol. Macromol.* **1989**, *11*, 339.
[4] W. Helbert, H. Chanzy, *Int. J. Biol. Macromol.* **1994**, *16*, 207.
[5] C. G. Biliaderis, C. M. Page, L. Slade, R. R. Sirett, *Carbohydr. Polym.* **1985**, *5*, 367.
[6] G. G. Gelders, H. Goesaert, J. A. Delcour, *Biomacromolecules* **2005**, *6*, 2622.
[7] S. Ahmadi-Abhari, A. J. J. Woortman, R. J. Hamer, A. A. C. M. Oudhuis, K. Loos, *Carbohydr. Polym.* **2013**, *93*, 224.
[8] F. F. Mikus, R. M. Hixon, R. E. Rundle, *J. Am. Chem. Soc.* **1946**, *68*, 1115.
[9] H. F. Zobel, A. D. French, M. E. Hinkle, *Biopolymers* **1967**, *5*, 837.
[10] G. F. Fanta, C. L. Swanson, W. M. Doane, *J. Appl. Polym. Sci.* **1990**, *40*, 811.
[11] R. L. Shogren, R. V. Greene, Y. V. Wu, *J. Appl. Polym. Sci.* **1991**, *42*, 1701.
[12] R. L. Shogren, A. R. Thompson, R. V. Greene, S. H. Gordon, G. Cote, *J. Appl. Polym. Sci.* **1991**, *42*, 2279.
[13] R. L. Shogren, *Carbohydr. Polym.* **1993**, *22*, 93.
[14] J. Kadokawa, Y. Kaneko, A. Nakaya, H. Tagaya, *Macromolecules* **2001**, *34*, 6536.
[15] J. Kadokawa, Y. Kaneko, H. Tagaya, K. Chiba, *Chem. Commun.* **2001**, 449.
[16] J. Kadokawa, Y. Kaneko, S. Nagase, T. Takahashi, H. Tagaya, *Chem. Eur. J.* **2002**, *8*, 3321.
[17] J. Kadokawa, A. Nakaya, Y. Kaneko, H. Tagaya, *Macromol. Chem. Phys.* **2003**, *204*, 1451.

[18] Y. Kaneko, J. Kadokawa, *Chem. Rec.* **2005**, *5*, 36.
[19] T. Kida, T. Minabe, S. Okabe, M. Akashi, *Chem. Commun.* **2007**, 1559.
[20] Y. Kaneko, K. Beppu, J. Kadokawa, *Macromol. Chem. Phys.* **2008**, *209*, 1037.
[21] Y. Kaneko, T. Kyutoku, N. Shimomura, J. Kadokawa, *Chem. Lett.* **2011**, *40*, 31.
[22] M. Tusch, J. Krüger, G. J. Fels, *Chem. Theory Comput.* **2011**, *7*, 2919.
[23] J. Kadokawa, *Polymers* **2012**, *4*, 116.
[28] J. van der Vlist, M. Faber, L. Loen, T. J. Dijkman, L. A. T. W. Asri, K. Loos, *Polymers* **2012**, *4*, 674.
[29] J. Ciric, J. Oostland, J. W. de Vries, A. J. J. Woortman, K. Loos, *Anal. Chem.* **2012**, *84*, 10463.
[30] J. Ciric, K. Loos, *Carbohydr. Polym.* **2013**, *93*, 31.
[31] R. E. Rundle, D. French, *J. Am. Chem. Soc.* **1943**, *65*, 1707.
[32] A. Buléon, M. M. Delage, J. Brisson, H. Chanzy, *Int. J. Biol. Macromol.* **1990**, *12*, 25.
[33] T. J. Schoch, *J. Am. Chem. Soc.* **1942**, *64*, 2957.
[34] C. Heinemann, F. Escher, B. Conde-Petit, *Carbohydr. Polym.* **2003**, *51*, 159.
[35] Q. Zhang, Z. Lu, H. Hu, W. Yang, P. E. Marszalek, *J. Am. Chem. Soc.* **2006**, *128*, 9387.
[36] J. L. Putaux, M. B. Cardoso, D. Dupeyre, M. Morin, A. Nulac, Y. Hu, *Macromol. Symp.* **2008**, *273*, 1.
[37] M. C. Godet, V. Tran, P. Colonna, A. Buleon, M. Pezolet, *Int. J. Biol. Macromol.* **1995**, *17*, 405.
[38] B. Biais, P. Le Bail, P. Robert, B. Pontoire, A. Buléon, *Carbohydr. Polym.* **2006**, *66*, 306.
[39] C. Rondeau-Mouro, P. L. Bail, A. Buléon, *Int. J. Biol. Macromol.* **2004**, *34*, 309.
[40] M. B. Cardoso, J. L. Putaux, Y. Nishiyama, W. Helbert, M. Hÿtch, N. P. Silveira, H. Chanzy, *Biomacromolecules* **2007**, *8*, 1319.
[41] G. Rappenecker, P. Zugenmaier, *Carbohydr. Res.* **1981**, *89*, 11.
[42] J. Kawada, R. H. Marchessault, *Starch/Stärke* **2004**, *56*, 13.
[43] L. C. López, G. L. Wilkes, *Polymer* **1988**, *29*, 106.